ELSEVIER

Biochimica et Biophysica Acta 1240 (1995) 159–166

BBA Biochimica et Biophysica Acta

Osmotic permeability in a molecular dynamics simulation of water transport through a single-occupancy pore

Susana G. Kalko [a], Julio A. Hernández [b], J. Raúl Grigera [a], Jorge Fischbarg [c,*]

[a] *Instituto de Física de Líquidos y Sistemas Biológicos, Universidad Nacional de La Plata, La Plata, Argentina*
[b] *Sección Biofísica, Facultad de Ciencias, Universidad de la República, 11200 Montevideo, Uruguay*
[c] *Departments of Physiology and Cellular Biophysics, and Ophthalmology, College of Physicians and Surgeons, Columbia University, 630 West 168th Street, New York, NY 10032, USA*

Received 18 April 1995; accepted 20 July 1995

Abstract

The aim of this work is to determine plausible values for the rate constants of kinetic models representing water transport through narrow pores. We present here the results of molecular dynamics simulations of the movement of water molecules through a single-site hydrophilic pore. The system consists of a rectangular box of water molecules, some of which are positionally restrained so as to act as a membrane. This membrane separates two compartments where water molecules move freely; one of the positions in the membrane is initially vacant (the 'single-site pore'), but can be occupied by mobile molecules. To analyze the results, we represented the pore by a two-state kinetic diagram in which the vacant and occupied states are linked by transitions corresponding to the binding and release of water molecules. The mean occupancy and vacancy times directly yield the rate constants of binding and release, which in turn yield the osmotic water permeability coefficient per pore p_f. We also compute the apparent activation energies ΔE^* for the rate constants and for p_f. The p_f value was $(1.56 \pm 0.04) \cdot 10^{-11}$ cm^3/s (at 307 K), which is much larger than those determined for CHIP28 and for gramicidin A (of about 10^{-13} and 10^{-14} cm^3/s, respectively). These values were compared with those arising from a model of a symmetric single-file pore through which one-vacancy-mediated water transport takes place. The model yields an expression for p_f as a function of the rate constants and of the number of molecular positions (n) in the file. When $n = 1$, this expression becomes the one corresponding to the single-site pore studied in our current simulation. Using the rate constants of binding and release derived from our simulation, the p_f values are consistent with an occupancy value of 5–6 found for gramicidin A, and with occupancies of 4–7 that can be estimated for the single-file pore of a recently proposed model for CHIP28. ΔE^* for p_f is 3.0 kcal/mol, a value similar to that determined for CHIP28. Hence, the system simulated here appears plausible and can be used to mimic some physical properties of water transport through biological pores.

Keywords: Water pore; Osmotic permeability; Molecular dynamics simulation; Single file; Kinetic model

1. Introduction

The single-file mechanism has been diversely employed in theoretical models to interpret ionic conductance [1–3] and water permeability [4–9], and in molecular dynamics simulations [10–13] of narrow pores. Theoretical analysis of molecular models of single-file transport use kinetic, thermodynamic or dynamic formalisms, and yield expressions for the permeability coefficients for water. However, this analysis necessarily assumes a particular physical model for the transport process, the plausibility of which cannot be determined by the analysis per se. Computer simulations of the molecular dynamics of transport through membrane pores provide numerical results with which the applicability of the model can be evaluated, but no analytical expressions to describe general properties. In part due to these methodological particularities, the molecular nature of the processes of water movement inside narrow pores still remains unresolved [9,11]. Hence, a combination of these two approaches may contribute to clarify the subject.

In previous work, we developed kinetic models to describe pore-mediated water transport [7–9]. Our present work intends to determine plausible numerical values for the rate constants governing this class of models. For this,

* Corresponding author. Fax: +1 (212) 3052461; e-mail: fischbarg@cuccfa.ccc.columbia.edu.

SSDI 0005-2736(95)00187-5

we study a 'complete' system of water permeation consisting of two aqueous compartments separated by a membrane containing a hydrophilic pore. This paper deals with the simplest arrangement conceivable, namely, a single-occupancy pore.

To this end, we apply a combination of (a) molecular dynamics simulation of water transport and (b) kinetic analysis of the simulated system. We examine the exchange of molecules between two identical compartments containing only water molecules and separated by a membrane which has a single-occupancy hydrophilic pore. Throughout the simulation, the 'pore' can either be occupied by a water molecule, or vacant; we obtained the mean times of the occupied and vacant states at different temperatures. The simulation was described by a two-state kinetic diagram (Appendix A). We derived from it an expression for the permeability coefficient as a function of the rate constants; these were determined from the mean times for the occupied and vacant states. The activation energy for the osmotic permeability coefficient found here is similar to the one previously determined for CHIP28 [14,15]. Furthermore, the osmotic permeability coefficient obtained here is consistent with values derived from theoretical analysis of single-file transport applied to our simulation and to CHIP28 and gramicidin A (Appendix B). These studies have been presented in preliminary form at the 39th Annual Meeting of the U.S. Biophysical Society (1995).

2. Methods

Molecular dynamics simulations were performed using a modified version of the GROMOS package [16] in which the equation of motion was integrated using a leapfrog algorithm. The simulation box was rectangular; its initial dimensions were $4.243 \times 1.470 \times 1.153$ nm, with its longest side along the x-axis. About halfway along the x axis a roughly monomolecular water layer was located ('the membrane'), and was arranged in an expanded ice Ih structure so as to present a hydrophilic surface with a regular distribution of hydrogen-bonding sites. The oxygen-oxygen distance was chosen as 0.290 nm (in contrast to the 0.270 nm of ice Ih) to match the water structure. This choice was based on suggestions that biological membranes may have H-bonding sites distributed so as to match the average structure of the surrounding water [17,18]. These water molecules (except one) were positionally restrained with a harmonic potential. As a consequence, during simulation these molecules could vibrate around their position but could not leave their place. One molecule in the middle of this 'membrane' was left unrestrained, thereby generating a one-site hydrophilic pore in it. The rest of the box was filled randomly with water molecules.

Periodic boundary conditions were applied along all box faces; as a consequence, the two regions separated by the membrane were connected through periodicity restraints, so that exactly the same conditions applied to both. Fig. 1A shows a scheme of the simulation box.

In GROMOS the pressure is controlled by coupling the system to a hydrostatic bath. As the simulation develops, the positions of the walls of the box and the atomic coordinates of the water molecules are adjusted to preserve the internal pressure close to the reference pressure selected. A relaxation parameter is imposed to avoid instability. In our case we did not want to change the membrane lattice dimensions, so only the walls perpendicular to the x-axis were moved. Such anisotropic adjustment may produce some undesired pressure effects, but in any case these will disappear when the system reaches equilibrium. The reference pressure was selected as 101 325 Pa (1 atm). By coupling the system to a thermal bath, the temperature was controlled, which allowed the running of simulations at different temperatures. The details of the algorithm implemented in GROMOS to handle constant pressure and constant temperature have been priorly described [19].

Water was modeled with the SPC/E model [20,19]. SPC/E water, besides its computational merit, accounts for many properties of liquid water. Particularly relevant to our case is the fact that SPC/E reproduces the self diffusion coefficient and density much better than most of the models devised for liquid water [21]. The SPC/E water model has bond lengths and bond angles which are rigid. They were fixed using the procedure SHAKE [22] implemented in GROMOS.

A total number of 180 water molecules were included in the box, of which 17 were immobilized to form the membrane described above. For each temperature the system was allowed to equilibrate for 20 ps, which is far more than necessary to reach equilibrium. Since a constant-temperature constant-pressure algorithm is no longer conservative, total energy is not always conserved. However, when the system is in equilibrium the only possible exchange of energy would arise from numerical artifacts. Therefore, it was possible to check for equilibrium by monitoring the constancy of the total energy and of the box volume.

At each selected temperature the system was run for 100 ps after the equilibration period, using a time step of 1 fs. Trajectories were collected each time step for further analysis. The state of the site was ascertained after each step; molecules were taken to occupy the site if the center of their oxygens fell within a sphere of 0.2 nm diameter centered in the position of the center of the oxygen atom of the only molecule that had been left unrestrained among those in the membrane.

2.1. Kinetic models

The simulation results were analyzed employing a kinetic model of a single site pore (Fig. 1B). We describe the details of the kinetic treatment in Appendix A. We subsequently derive a general expression for the osmotic perme-

ability coefficient of a single-file symmetric pore in Appendix B.

3. Results

Using the trajectories, we monitored whether the site was occupied or vacant. By an appropriate housekeeping procedure, the average time for each state was recorded. If the sampling time had been longer than the shortest occupancy (or vacancy) times, the computed residency times would have been incorrect. Therefore, we obtained a series of preliminary runs using different sampling times. We found that 1 fs was short enough to avoid such shortcomings at the highest temperature studied, and used that as our sampling interval.

Fig. 2 shows histograms of the distributions of occupancy times at 307.05 and 356.16 K. As shown there, the distributions can be fitted by single exponentials, as is characteristic of a Markovian process [23–26]. To obtain an estimate of the errors for the mean occupancy and vacancy times, we first computed the overall average times for the entire data set from a 100 ps run, and then subdivided such run into 50 subsets of 2 ps each, and

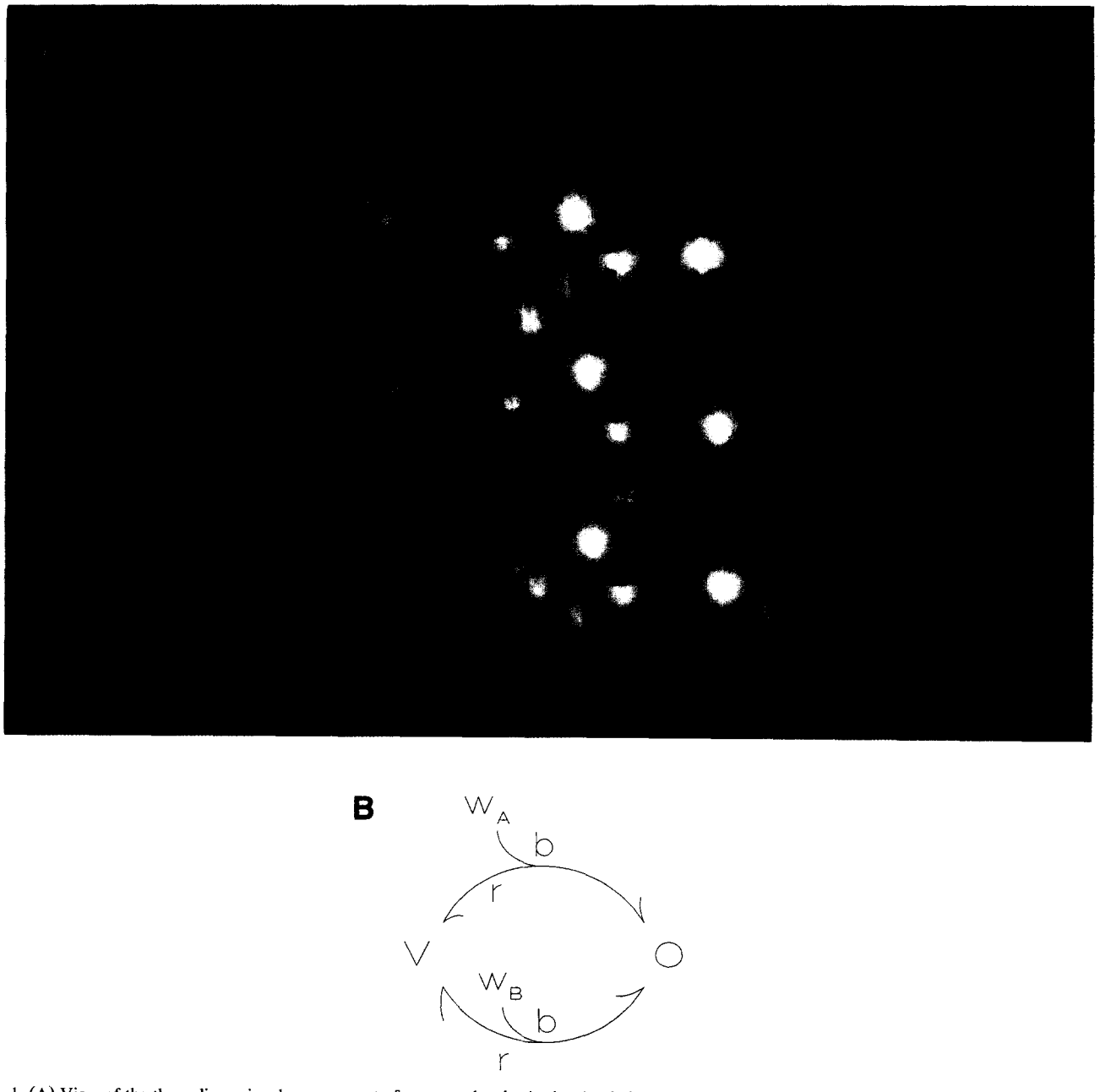

Fig. 1. (A) View of the three-dimensional arrangement of water molecules in the simulation box at a given time. The molecules immobilized and forming part of the 'ice-water' membrane are highlighted. (B) Kinetic model corresponding to the simulation. See Appendix A for the meaning of the symbols.

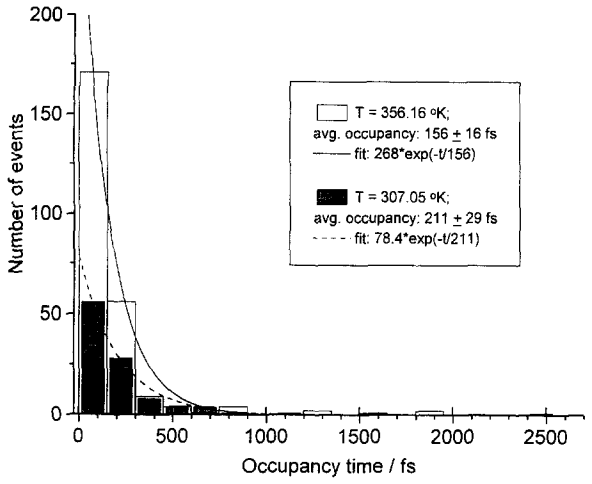

Fig. 2. Histogram depicting the distribution of the occupancy times at the two temperatures given. The abscissa (x) represents the duration of time intervals (bin size: 75 fs) for which the pore was occupied, and the ordinate (y) the frequency of occupation events. As stated in the text, runs lasted 100 ps and time steps were 1 fs. The mean values ($\langle\tau\rangle$) reported for each temperature in the text result from: $\langle\tau\rangle = \Sigma xy/\Sigma y$. Here and in Fig. 3, the errors are calculated as detailed in the text.

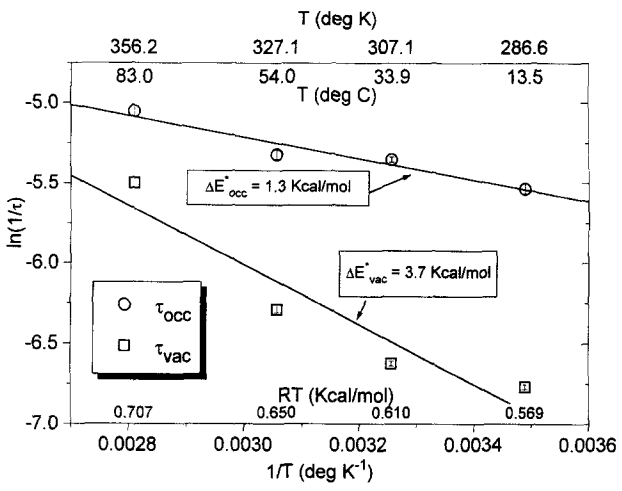

Fig. 4. The logarithm of the inverse of the mean occupancy and vacancy times versus the inverse of the temperature (Arrhenius plot). The top axis labels are corresponding Kelvin and Celsius values. Values by the bottom axis represent the energy of thermal agitation at the experimental temperatures sampled. The activation energies given correspond to the slopes indicated (slope × R).

obtained the average times for each subset. Since by the Central Limit Theorem the subset averages are expected to follow a Gaussian distribution [27], these averages together with the overall average were used to determine the standard deviations of the overall means.

Fig. 3 shows stacked columns representing the average vacancy and occupation times plotted against absolute temperature. Both times decrease with increasing temperature, but the decrease in vacancy times is much more pronounced.

In Fig. 4, the data of Fig. 3 are plotted as logarithms of the inverse of average vacancy and occupation times against the inverse of absolute temperature. Linear fits are shown.

According to the kinetic model described in detail in Appendix A, the unitary osmotic permeability for the single-site pore considered here is given by Eq. (A7):

$$(p_f)_{eq} = rb/(2(r + bw))$$

where $(p_f)_{eq}$ is the equilibrium permeability per pore, r is the release constant, b is the binding constant, and w is the solvent activity (55.55 mol/l), as detailed in Appendix A. Table 1 shows the values for the permeability and rate constants at different temperatures.

Fig. 5 shows the logarithm of the permeability plotted against the inverse of absolute temperature. From this Arrhenius plot, we obtain for the activation energy a value of (slope times gas constant R):

$$\Delta E^*_{act} = 3.0 \text{ kcal/mol}$$

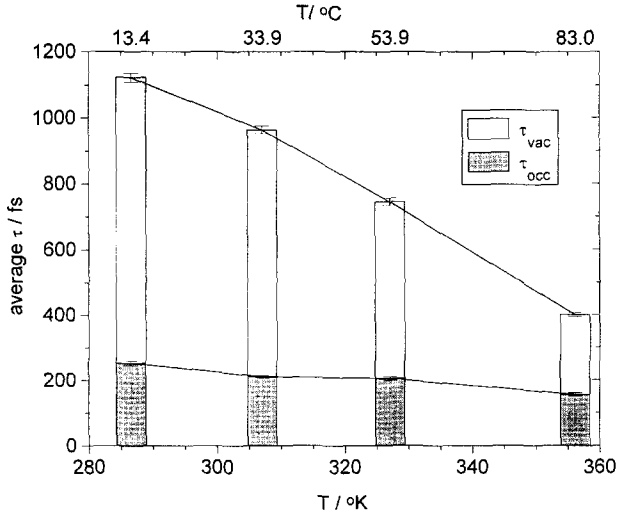

Fig. 3. Mean vacancy and occupancy times stacked in columns at four different temperatures.

4. Discussion

4.1. The single-file model for water transport through biological pores

The system best characterized for theoretical and experimental studies on ionic and water movements through

Table 1
Permeability and rate constant values at different temperatures

Temperature (K)	Binding constant b (10^{13} cm^3/(mol s))	Release constant r (10^{12} s^{-1})	Unitary osmotic permeability p_f (10^{-11} cm^3 s^{-1})
286.610	2.068 ± 0.032	3.949 ± 0.118	1.335 ± 0.055
307.050	2.393 ± 0.037	4.733 ± 0.079	1.557 ± 0.041
327.110	3.336 ± 0.068	4.875 ± 0.131	2.014 ± 0.079
356.160	7.355 ± 0.191	6.400 ± 0.213	3.741 ± 0.179

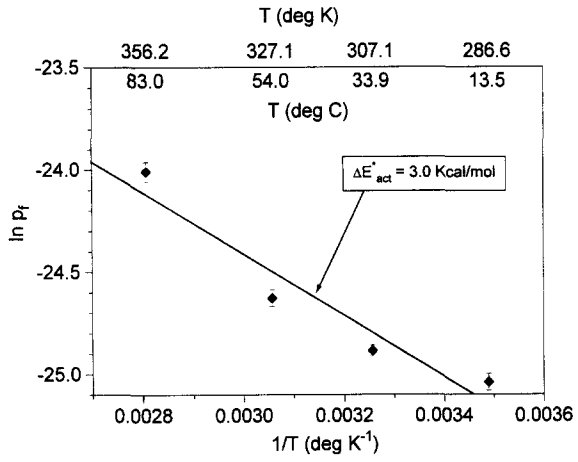

Fig. 5. Arrhenius plot of the unitary osmotic permeability values. Other details as in Fig. 4.

channels of molecular dimensions across lipid bilayer membranes is the pore formed by the antibiotic polypeptide gramicidin A (for reviews, see [28,29]). Structural evidence [28,30] shows that the gramicidin A pores have a narrow diameter uniform along their length, which suggests the presence of a single file of molecules in the pore. The values reported for the osmotic permeability coefficient of gramicidin A (per pore) range from $6 \cdot 10^{-14}$ cm^3/s [31] to $1 \cdot 10^{-14}$ cm^3/s [32], as discussed by Finkelstein ([28], p. 139).

In many types of cells, water movement across their plasma membranes takes place through integral proteins. The most representative of such proteins are the erythrocyte CHIP28 water channel protein [33] and other water channel members of the MIP family [34–37]. Several other integral membrane proteins have also been demonstrated to constitute, albeit to a lesser degree, sites of transmembrane water transport [38–42]. For CHIP28 protein molecules reconstituted into liposomes, their unitary osmotic permeability coefficient is about 10^{-13} cm^3/s [14]. To be noted, kidney and erythrocyte water channel monomers have been shown to form functional water channels [15,43–45]. Water channel proteins have been classically assumed to conform to a single-file model of water transport [28,46]. This presumption appears logical, since water channel proteins are very specific for water [46], and a pore diameter that would allow the permeation of molecules larger than water would make such specificity difficult to explain. Except for the case of gramicidin A, there is still no structural evidence to support the single-file model for water channel membrane proteins. A structural model has recently been proposed for proteins belonging to the MIP family by using predictive computational algorithms [47]. According to such model, water channels may resemble porins, for which the channel region is formed by the inside of a transmembrane β-barrel, and is narrowed by a loop that winds its way into the pore ('restricted pore' model). In another conception [48], water channels would consist of transmembrane helices joined by relatively long loops that would impart the arrangement the cross section of an hourglass. In both models, the idealized water pore would hence consist of two relatively wide segments in free communication with the surrounding environments connected by a narrower region through which water movements would be constrained. We propose that water might move in single file through such constriction; of course, the single-file zone could include more than one occupancy site for water molecules. Using porins for an estimate (Van der Waals barrel inside diameter 15–25 Å), the wide segments would be relatively large. Again for porins, its loop L3 restricts its diameter and contributes to delimit a pore. According to molecular dynamics simulations, such loop has flexible zones that allow it to display mobility high enough to close the pore [49,50]; in such context, the single-file zone and its occupancy modes might vary as the loop fluctuates.

4.2. Theoretical interpretation of the numerical results obtained in the simulation

As mentioned above, the value of the permeability coefficient obtained for the single-site pore in the present simulation is 2 and 3 orders of magnitude larger than those experimentally determined for CHIP28 and gramicidin A, respectively. Among other reasons, this difference may be explained by: (a) occupancy number, and (b) channel structure.

4.2.1. Occupancy number

Diverse theoretical analysis of single-file water transport [4,6,7] yield expressions for the permeability coefficients. In every case, from such expressions, the permeability decreases with increasing pore length (or, equivalently, with the number of sites along the file). The extent of the decrease depends also on the molecular mechanism assumed for the transport process [7]. For the case of single-file transport under near-saturation conditions, kinetic models yield expressions for the osmotic permeability coefficients as functions of the rate constants, the water activities in the compartments, and the number of positions in the file [7]. Fig. 6a shows a particular case of a single-file water pore in which transport occurs via a one-vacancy mechanism. For this symmetric pore, only three different rate constants govern transport. In Appendix B we derive an expression for the osmotic permeability coefficient p_f corresponding to this case. In Fig. 6b we show p_f as a function of the total number of molecular positions (n) in the file. The values for the rate constants of binding and release were those obtained with our molecular dynamics simulation; three arbitrary values of the rate constant of displacement between sequential positions inside the pore were considered. In Fig. 6b, the value of p_f determined for $n = 1$ equals the one derived in the molecu-

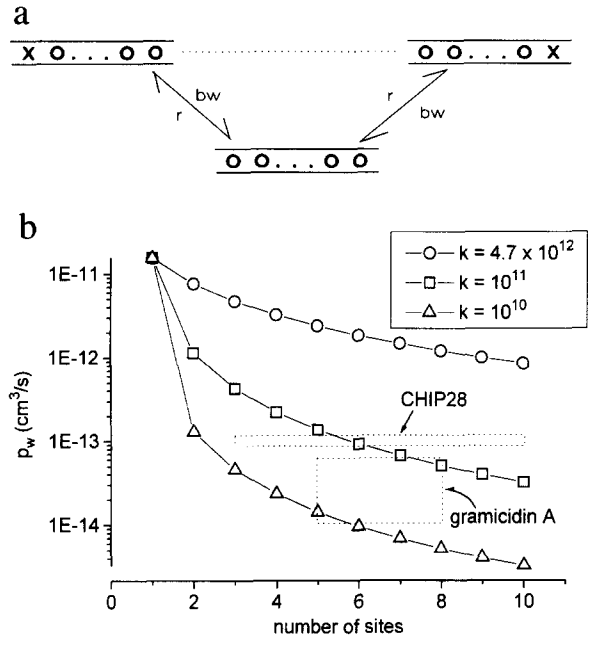

Fig. 6. (a) Kinetic model of one-vacancy-mediated transport of water through a symmetric single-file pore, under equilibrium conditions ($w_A = w_B = w$). Open circles: water molecules; X: vacant positions. The punctuated line represents a linear sequence of transitions between one-vacancy states. Each transition is governed by the same rate constant (k) in either direction. (b) Plot of p_f as a function of the number of positions n along the file, using Eq. (B2). For this plot, $b = 2.4 \cdot 10^{13}$ cm^3 mol^{-1} s^{-1}, $r = 4.7 \cdot 10^{12}$ s^{-1}, and $w = 0.055$ mol cm^{-3} (see also Table 1).

lar dynamics simulation, thus validating the general expression. Fig. 6b also highlights the possible regions of application of the analysis to pores of the type of CHIP28 and gramicidin A. The gramicidin A pore has been variously calculated to hold between 5 and 9 water molecules ([28], pp. 140–142); our analysis is thus consistent with these estimates. Our analysis also suggests that the putative single-file pore in CHIP28 would contain at most 6 sites, a value consistent with proposed structural models (see above). If the single-file symmetric pore with a one-vacancy-mediated transport mechanism represents a good model for this type of water pores, and if the molecular dynamics simulation performed here yields plausible values for the rate constants of binding and release to (from) the extreme positions of a water pore, Fig. 6b also predicts the range of the numerical values for the displacement rate constant. All the arguments in this section also lead us to propose that the single-site pore simulated here represents the case exhibiting the largest possible water permeability among narrow pores.

4.2.2. Channel structure

The physicochemical properties associated with the particular structure of a given protein channel may contribute to determine its permeability coefficient. If this represents a significant factor, the simple hydrophilic pore model studied here may inform on some of the essential characteristics relevant to actual water transport through biological membrane pores, but would still require further modifications to better mimic protein channels. Future work with progressively more complex simulation models may result in the information necessary to account for the characteristics of water passage through channel proteins.

4.3. Activation energies of osmotic permeability coefficients

The overall activation energy determined here for p_f is 3.0 kcal/mol, similar to the one determined for CHIP28 [14,15,14,15]. Values of activation energy reported for water channels tend to fall at or below 4.6 kcal/mol (corresponding to water self-diffusion, [51], p. 21]); some examples: 3.2 kcal/mol [52]; 2 kcal/mol [53]; 2–4 kcal/mol [54]. The similarity between such values and the activation energy found in our simulation further supports the plausibility of the model employed here.

Acknowledgements

This work was supported by the Consejo Nacional de Investigaciones Científicas of Argentina (CONICET), by USPHS NIH grants EY06178 and EY08918, and by Research to Prevent Blindness, Inc. (RPB). SGK had partial support from the Comisión de Investigaciones Científicas of the Province of Buenos Aires, Argentina; J.A.H. was supported by a Fulbright Comission Award and by an RPB Travel Fellowship.

Appendix A

A.1. Kinetic model of the molecular dynamics simulation

A.1.1. Relation between the mean occupancy and vacancy times, and the kinetic constants

The model of Fig. 1B represents a simple kinetic description of the molecular dynamics simulation performed here. The symbols used in what follows represent:

N_T: total mol of pores per unit area of the membrane ($N_T = V + O$)
V: mol of vacant pores per unit area of the membrane
O: mol of occupied pores per unit area of the membrane
w_A: water activity in compartment A (mol/unit volume)
w_B: water activity in compartment B (mol/unit volume)
b: kinetic constant of binding of water molecules (Hz unit volume/mol)
r: kinetic constant of release of water molecules (Hz)
J_v: water volume flow (volume per unit time and unit area)
V_w: molar volume of water
P_f: osmotic water permeability coefficient (length per unit time)

p_f: unitary (per pore) osmotic water permeability coefficient (volume per unit time)

N: Avogadro's number

As can be seen, we have assumed that a single kinetic constant of binding (release) determines the rate of molecule binding (release) from (to) any of the two compartments. This assumption is supported by the symmetrical character of the simulation box.

The net molar velocity v of the transition $V \leftrightarrow O$ is given by

$$v = b(w_A + w_B)V - 2rO \quad \text{(A1)}$$

For a system in equilibrium, $w_A = w_B = w$ and $v = 0$. Therefore, from Eq. (A1),

$$O/V = bw/r = K_{eq} \quad \text{(A2)}$$

For the monomolecular case represented by Eq. (A2), it can be demonstrated that [55]

$$\tau_O = r^{-1} \text{ and } \tau_V = (bw)^{-1} \quad \text{(A3)}$$

where τ_O and τ_V are the mean times spent by the system in states O and V, respectively. Therefore, from Eq. (A3), determinations of τ_O, τ_V and w yield values for the kinetic constants b and r.

A.1.2. Osmotic permeability coefficient

We use the algorithmic method developed by Hill [55] to derive a steady-state expression for the net water flux between the compartments. Since there is only one cycle, the following relations apply:

$$V = N_T(2r/\Sigma)$$

$$O = N_T b(w_A - w_B)/\Sigma$$

Σ is the sum of all the directional diagrams, given by:

$$\Sigma = 2r + b(w_A + w_B) \quad \text{(A4)}$$

To calculate the net flux of water across the membrane, it is illustrative to redraw the kinetic scheme as:

$$A \underset{rO}{\overset{bw_A V}{\rightleftarrows}} O \underset{bw_B V}{\overset{rO}{\rightleftarrows}} B$$

The net molar flux of water (say from A to B) per unit area M_{AB} is then:

$$M_{AB} = bw_A V - rO = rO - bw_B V$$

Using Eqs. (A4), we obtain:

$$M_{AB} = ((N_T rb)/\Sigma)(w_A - w_B) \quad \text{(A5)}$$

As can be seen, the 'symmetrical' character of the pore with respect to the kinetic constants already implies the condition of detailed balance.

Eq. (A5) can be rewritten as:

$$M_{AB}V_w = J_v = ((N_T rb)/\Sigma)V_w(w_A - w_B) = P_f V_w(w_A - w_B)$$

Since N_T = (number of pores/(N · unit area)), the osmotic water permeability coefficient per pore is given by

$$p_f = P_f/(\text{number of pores/unit area}) = rb/(N\Sigma) \quad \text{(A6)}$$

For the particular case of equilibrium ($w_A = w_B = w$), p_f becomes the 'equilibrium' permeability coefficient per pore $(p_f)_{eq}$, given by

$$(p_f)_{eq} = rb/(N\Sigma_{eq}) = rb/(2N(r + bw)) \quad \text{(A7)}$$

Appendix B

B.1. Model of a symmetric single-file water pore

Here we derive an expression for the steady-state osmotic permeability coefficient P_f corresponding to the pore model of Fig. 6a. The derivation can also be done from the expression for P_f from the general kinetic model of one-vacancy mediated water transport through a single-file pore [7]. Again, we employ the diagrammatic method developed by Hill [55]. As shown in Fig. 6a, aside from the binding and release constants b and r, another rate constant governs the kinetics, the displacement constant k. N_T, N and w have the same meanings as in Appendix A, n is the total number of molecule positions in the file.

Since there is only one cycle, the permeability coefficient is given by

$$P_f = N_T \Pi/\Sigma \quad \text{(B1)}$$

where, from the detailed balance condition,

$$\Pi = brk^{n-1}$$

and where Σ is the sum of all the directional diagrams of the model, and is given by

$$\Sigma = 2k^{n-1}(nr + bw) + (n-1)k^{n-2}(nrbw + (bw)^2)$$

Hence, for the model of Fig. 6a, the osmotic permeability coefficient per pore is given by

$$p_f = P_f/(N_T N) \quad \text{(B2)}$$

References

[1] Kohler, H.-H. and Heckmann, K. (1979) J. Theor. Biol. 79, 381–401.
[2] Kohler, H.-H. and Heckmann, K. (1980) J. Theor. Biol. 85, 575–595.
[3] Schumaker, M.F. and MacKinnon, R. (1990) Biophys. J. 58, 975–984.
[4] Levitt, D.G. (1974) Biochim. Biophys. Acta 373, 115–131.
[5] Levitt, D.G. (1984) Curr. Top. Membr. Transp. 21, 181–197.
[6] Finkelstein, A. and Rosenberg, P.A. (1979) in Membrane Transport Processes (Stevens, C.F. and Tsien, R.W., eds.), Vol. 3, pp. 73–88, Raven Press, New York, NY.
[7] Hernandez, J.A. and Fischbarg, J. (1992) J. Gen. Physiol. 99, 645–662.
[8] Hernandez, J.A. and Fischbarg, J. (1994) Biophys. J. 67, 996–1006.
[9] Hernandez, J.A. and Fischbarg, J. (1994) Biophys. J. 67, 1464–1472.
[10] Chiu, S.-W., Jakobsson, E., Subramaniam, S. and McCammon, J.A. (1991) Biophys. J. 60, 273–285.

[11] Chiu, S.-W., Novotny, J.A. and Jakobsson, E. (1993) Biophys. J. 64, 98–108.
[12] Roux, B. and Karplus, M. (1991) Biophys. J. 59, 961–981.
[13] Roux, B. and Karplus, M. (1994) Annu. Rev. Biophys. Biomol. Struct. 23, 731–761.
[14] Zeidel, M.L., Ambudkar, S.V., Smith, B.L. and Agre, P. (1992) Biochemistry 31, 74–7440.
[15] Agre, P., Preston, G.M., Smith, B.L., Jung, J.S., Raina, S., Moon, C., Guggino, W.B. and Nielsen, S. (1993) Am. J. Physiol. 265, F463–F476.
[16] Van Gunsteren, W.F. and Berendsen, H.J.C. (1975) GROningen MOlecular Simulation, BIOMOS, Nijenborgh 16, 9747 AG Groningen, The Netherlands.
[17] Warner, D.T. (1962) Nature 196, 1052–1055.
[18] Donnamaria, M.C., Howard, E.I. and Grigera, J.R. (1994) Faraday Trans. 90, 2731–2735.
[19] Berendsen, H.J.C., Postma, J.P.M., Van Gunsteren, W.F., Di Nola, A. and Haak, J.R. (1984) J. Chem. Phys. 81, 84–90.
[20] Berendsen, H.J.C., Grigera, J.R. and Straatsma, T.P. (1987) J. Phys. Chem. 91, 6169–6271.
[21] Finney, J.L., Quinn, J.E. and Baum, J.O. (1985) Water Sci. Rev. 1, 93–170.
[22] Ryekaert, J.P., Cicotti, G. and Berendsen, H.J.C. (1977) J. Comput. Phys. 23, 327–341.
[23] Colquhoun, D. and Hawkes, A.G. (1981) Proc. R. Soc. Lond. B Biol. Sci. 211, 205–235.
[24] Horn, R. and Lange, K. (1983) Biophys. J. 43, 207–223.
[25] Colquhoun, D. and Sigworth, F.J. (1983) in Single Channel Recording (Sackman, B. and Neher, E., eds.), Plenum Press, New York.
[26] Kienker, P. (1989) Proc. R. Soc. Lond. B Biol. Sci. 2, 269–309.
[27] Feller, W. (1971) An Introduction to Probability Theory and its Applications, Vol. II, John Wiley, New York.
[28] Finkelstein, A. (1987) Water movement through lipid bilayers, pores, and plasma membranes. Theory and reality. In Distinguished Lecture series of the Society of General Physiologists, Vol. 4, John Wiley, New York.
[29] Hille, B. (1992) Ionic Channels of Excitable Membranes, 2nd. Edn., Sinauer Associates, Sunderland.
[30] Urry, D.W. (1971) Proc. Natl. Acad. Sci. USA 68, 672–676.
[31] Dani, J.A. and Levitt, D.G. (1981) Biophys. J. 35, 485–500.
[32] Rosenberg, P.A. and Finkelstein, A. (1978) J. Gen. Physiol. 72, 327–340.
[33] Preston, G.M., Carroll, W.B., Guggino, W.B. and Agre, P. (1992) Science 256, 385–387.
[34] Fushimi, K., Uchida, S., Hara, Y., Hirata, Y., Marumo, F. and Sasaki, S. (1993) Nature 1, 549–552.
[35] Zhang, R., Skach, W., Hasegawa, H., Van Hoek, A.N. and Verkman, A.S. (1993) J. Cell Biol. 120, 359–369.
[36] Maurel, C., Reizer, J., Schroeder, J.I. and Chrispeels, M.J. (1993) EMBO J. 12, 2241–2247.
[37] Abrami, L., Simon, M., Rousselet, G., Berthonaud, V., Buhler, J.-M. and Ripoche, P. (1994) Biochim. Biophys. Acta 1192, 147–151.
[38] Dani, J.A. (1989) J. Neurosci. 9, 884–892.
[39] Fischbarg, J., Kuang, K., Vera, J.C., Arant, S., Silverstein, S.C., Loike, J. and Rosen, O.M. (1990) Proc. Natl. Acad. Sci. USA 87, 3244–3247.
[40] Fischbarg, J., Kuang, K., Li, J., Arant-Hickman, S., Vera, J.C., Silverstein, S.C. and Loike, J.D. (1993) in Proc. Alfred Benzon Symposium 34, Water transport in leaky epithelia (Ussing, H.H., Fischbarg, J., Sten Knudsen, E., Hviid Larsen, E. and Willumsen, N.J., eds.), pp. 432–446, Munksgaard, Copenhagen.
[41] Zhang, R., Alper, S., Thorens, B. and Verkman, A.S. (1991) J. Clin. Invest. 88, 1553–1558.
[42] Hasegawa, H., Skach, W., Baker, O., Calayag, M.C., Lingappa, V. and Verkman, A.S. (1992) Science 258, 1477–1479.
[43] Van Hoek, A.N., Hom, M.L., Luthjens, H., De Jong, M.D., Dempster, J.A. and Van Os, C.H. (1991) J. Biol. Chem. 266, 16633–16635.
[44] Van Hoek, A.N., Luthjens, H., Hom, M.L., Van Os, C.H. and Dempster, J.A. (1992) Biochem. Biophys. Res. Commun. 184, 1331–1338.
[45] Shi, L.B., Skach, W. and Verkman, A.S. (1994) J. Biol. Chem. 269, 10417–10422.
[46] Macey, R.I. (1984) Am. J. Physiol. 246, C195–C203.
[47] Fischbarg, J., Li, J., Cheung, M., Czegledy, F., Iserovich, P. and Kuang, K. (1995) J. Memb. Biol. 143, 177–188.
[48] Jung, J.S., Preston, G.M., Smith, B.L., Guggino, W.B. and Agre, P. (1994) J. Biol. Chem. 269, 14648–14654.
[49] Björksten, J., Soares, C.M., Nilsson, O. and Tapia, O. (1994) Prot. Eng. 7, 487–493.
[50] Soares, C.M., Björksten, J. and Tapia, O. (1995) Prot. Eng. 8, 5–12.
[51] House, C.R. (1974) Water transport in cells and tissues, Edward Arnold, London.
[52] Whittembury, G., Carpi-Medina, P., Gonzalez, E. and Linares, H. (1984) Biochim. Biophys. Acta 775, 365–373.
[53] Echevarría, M. (1990) PhD. Thesis, Simón Bolívar University, Caracas, Venezuela.
[54] Echevarría, M., Frindt, G., Preston, G.M., Milovanovic, S., Agre, P., Fischbarg, J. and Windhager, E.E. (1993) J. Gen. Physiol. 101, 827–841.
[55] Hill, T.L. (1977) Free Energy Transduction in Biology, Academic Press, New York.